Supporting Information

Incorporation of spirobifluorene regioisomers in electron-donating molecular systems for organic solar cells

Ibrahim Bulut,[a] Patricia Chávez,[a] Sadiara Fall,[b] Stéphane Méry,[c] Benoit Heinrich,[d] Joëlle Rault-Berthelot,[d] Cyril Poriel,*[d] Patrick Lévêque,*[c] and Nicolas Leclerc*[a]

Table of contents

[a] Institut de Chimie et Procédés pour l'Energie, l'Environnement et la Santé (ICPEES), Département d'Ingénierie Polymère, UMR 7515 associée au CNRS, Ecole Européenne de Chimie, Polymères et Matériaux, 25 rue Becquerel, 67087 Strasbourg, France, E-mail: leclercn@unistra.fr, Phone: (+33)3-6885-2709.

[b] Laboratoire ICube, Université de Strasbourg, CNRS, 23 rue du Loess, 67037 Strasbourg, France, Email:patrick.leveque@unistra.fr, Phone: (+33)3-8810-6294.

[c] Institut de Physique et de Chimie des Matériaux de Strasbourg, 23 rue du Loess, BP 84047, 67034 Strasbourg Cedex 02, France.

[d] UMR CNRS 6226 "Institut des Sciences Chimiques de Rennes", Université de Rennes 1-Campus de Beaulieu-35042 Rennes cedex France. E-mail: cyril.poriel@univ-rennes1.fr, Phone: (+33)2-2323-5977 or (+33)2-2323-5964.

Materials and methods

All reagents and chemicals were purchased from commercial sources. Xylene, dioxane and toluene were distilled from Na. Palladium catalysts, phosphines ligands and other reagents and chemicals were used as received. DPP-Thiophene,[S1] and 2/4-spirobifluorene mono-boronated[S2,S3] were prepared as described in the literature. ^{1}H and ^{13}C NMR spectra were recorded on 300 NMR spectrometer, with ^{1}H and ^{13}C chemical shifts reported in δ (ppm) relative to $CDCl_3$ (7.26 and 77.16 respectively) and CD_2Cl_2. (5.32 and 54.0) MS (EI) and Maldi-TOF experiments were performed on a Bruker spectrometer within the service centers at "Institut de Chimie" of Strasbourg University.
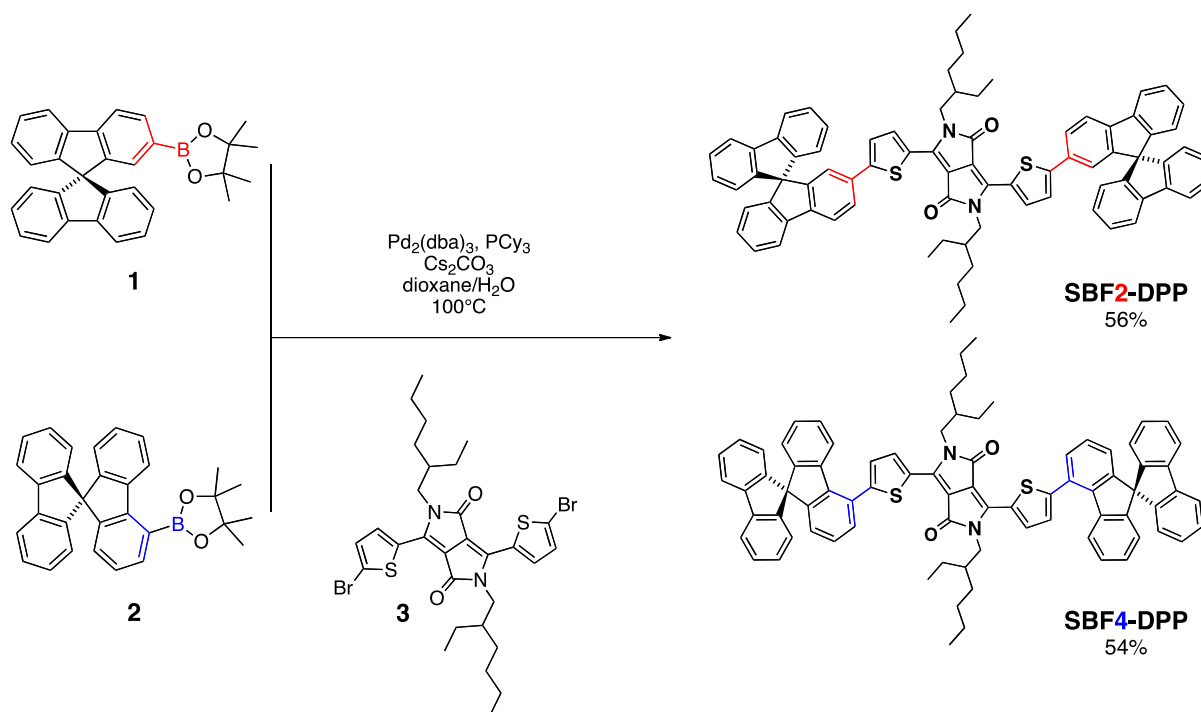

Figure S1: Synthesis of **SBF2-DPP** and **SBF4-DPP**

Suzuki cross-coupling procedure

A flame dried Schlenck was charged with di-brominated DPP-Thiophene (1.0 equiv). Degassed mixture solvent (0.1M) was added under inert gas followed by the appropriate mono-boron spirobifluorene (2.2 equiv). The base (2.2 equiv) was then added in one portion. Finally the palladium catalyst (0.03 equiv) and phosphine ligand (0.06 equiv) were added and the mixture was stirred 24 hours at 100°C. After cooling to room temperature the reaction mixtures were evaporated under reduced pressure and purified by column chromatography (silica gel, CH_2Cl_2/PE: 70/30).
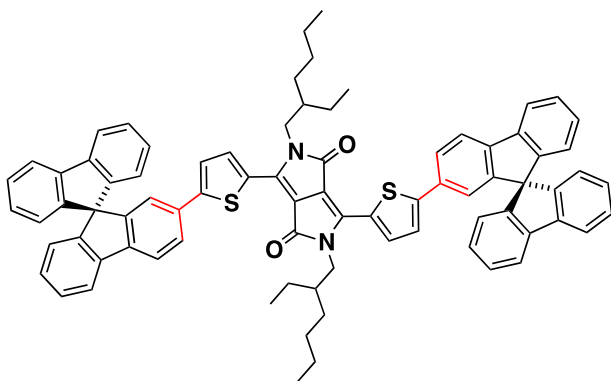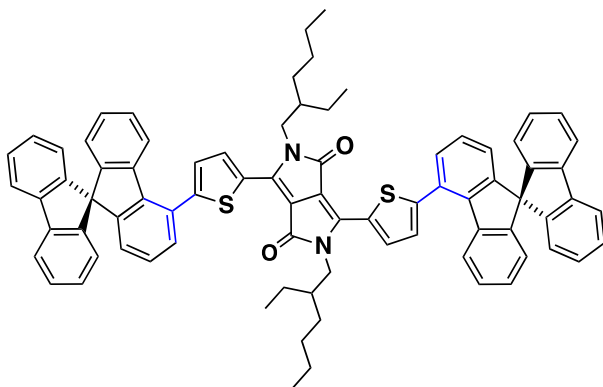
3-6-bis(5-(9,9'-spirobi[fluoren]-7-yl)thiophen-2-yl)-2,5-bis(2-ethylhexyl)pyrrolo[3,4-*c*]pyrrole-1,4(2*H*,5*H*)-dione **SBF2-DPP**

Molecular weight: 1153.5 g/mol. Blue solid. Yield: 56%

^{1}H NMR (300 MHz, CDCl$_3$) δ: 8.79 (d, *J* = 4.2 Hz, 1H), 7.88-7.84 (m, 4H), 7.69 (d, *J* = 7.9 Hz, 1H), 7.41-7.36 (m, 3H), 7.24 (d, *J* = 4.2 Hz, 1H), 7.12 (t, *J* = 7.5 Hz, 3H), 6.99 (pseudo s, 1H), 6.76 (d, *J* = 7.6 Hz, 2H), 6.72 (d, *J* = 7.6 Hz, 1H), 4.13 (pseudo d, *J* = 6.5 Hz, 2H), 1.85-1.75 (m, 1H), 1.30-1.16 (m, 8H), 0.88-0.77 (m, 6H).

^{13}C NMR (75 MHz, CDCl$_3$) δ: 161.7, 149.9, 149.6, 149.4, 148.2 (x2), 142.6, 141.8, 140.8, 139.6, 136.5, 132.8, 128.6, 128.4, 127.9 (x3), 127.9 (x2), 126.2, 124.1 (x3), 121.5, 120.6, 120.2, 120.1 (x3), 108.2, 66.0, 45.8, 39.1, 30.2, 28.3, 23.7, 23.0, 14.0, 10.6.

MS MALDI-TOF m/z calculated C$_{80}$H$_{69}$N$_2$O$_2$S$_2$[M-H$^+$]: 1153.479 g/mol; found [M-H$^+$]: 1153.450 g/mol.

3,6-bis(5-(9,9'-spirobi[fluoren]-5-yl)thiophen-2-yl)-2,5-bis(2-ethylhexyl)pyrrolo[3,4-*c*]pyrrole-1,4(2*H*,5*H*)-dione **SBF4-DPP**

Molecular weight: 1153.5 g/mol. Blue solid. Yield: 54%

^{1}H NMR (300 MHz, CD$_2$Cl$_2$) δ: 9.15 (d, *J* = 3.9 Hz, 1H), 7.89 (d, *J* = 7.5 Hz, 2H), 7.54 (d, *J* = 3.9 Hz, 1H), 7.40 (t, *J* = 7.2 Hz, 4H), 7.17-7.10 (m, 4H), 7.06 (d, *J* = 7.2 Hz, 1H), 6.78-6.73 (m, 3H), 6.68 (d, *J*

= 7.2 Hz, 1H), 4.13 (pseudo t, J = 6.5 Hz, 2H), 2.07-2.00 (m, 1H), 1.47-1.25 (m, 8H), 0.95-0.82 (m, 6H).

^{13}C NMR (75 MHz, CD$_2$Cl$_2$) δ: 162.1, 150.1, 149.3, 148.7 (x2), 147.6, 142.0 (x2), 141.0, 140.2, 140.1, 135.9, 131.0, 130.6, 128.7, 128.5, 128.2, 128.1 (x3), 128.0, 127.7, 127.4, 124.7, 123.9 (x3), 123.2, 120.3 (x2), 108.3, 65.8, 46.1, 39.4, 30.5, 28.6, 23.8, 23.2, 13.9, 10.4.

MS MALDI-TOF m/z calculated C$_{80}$H$_{69}$N$_2$O$_2$S$_2$[M-H$^+$]: 1153.479 g/mol; found [M-H$^+$]: 1153.450 g/mol.

UV-Visible Spectroscopy

Absorption spectra in solution and in thin films were recorded on a Shimadzu UV-2101 spectrophotometer. In solid state, the absorption spectra were measured on thin films drop-casted on glass substrates from a 0.5 mg/mL chloroform solution of SBF-based dyes.

Density Functional Theory calculations

Density functional theory (DFT) calculations have been performed using SPARTAN 10 (www.wavefun.com) at the B3LYP/6-311+G* level of theory in vacuum.

Starting from the optimized geometry calculated by DFT for SBF4-DPP, a rotation has been applied (red arrow in Figure S2) and the distance between hydrogen atom in the ortho position of the pendant thiophene ring and that of the phenyl unit of the fluorenyl core (position C5) has been calculated. This distance (d_{H-H}) as a function of the dihedral angle defined by the four highlighted C atoms (Figure S2) is represented in Figure S3.
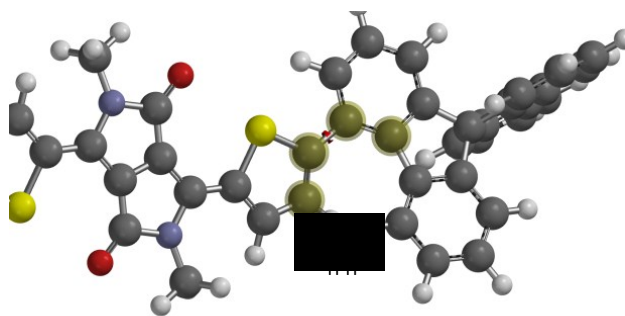

Figure S2: definition of the dihedral angle (highlighted C atoms) and rotation applied (black arrow) for the calculation of the d_{H-H} distance.
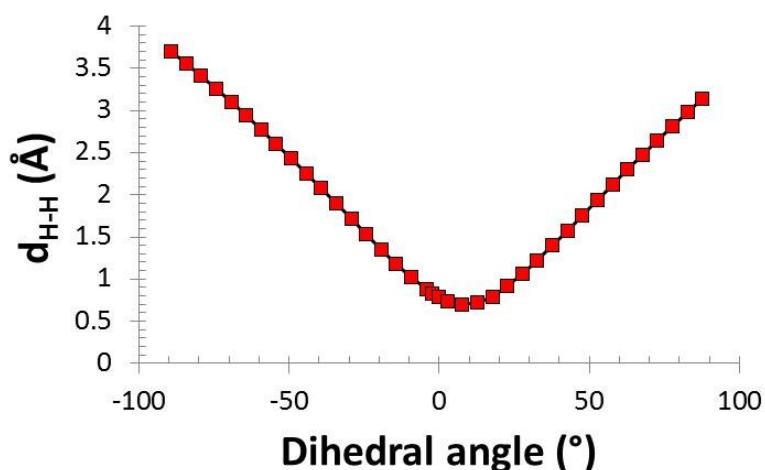
Figure S3: variation of d_{H-H} as a function of the dihedral angle as defined in Figure S2.

A value of -50° for the dihedral angle, in the same range as the angle between the mean "plane" of the central thiophene-DPP-thiophene core and that of the substituted fluorene unit of the SBF fragment in SBF4-DPP corresponds to a d_{H-H} distance of 2.435 Å. This value corresponds roughly to two times the van der Waals radius of the hydrogen atom confirming that the steric interaction observed in SBF4-DPP between the hydrogen atom in the ortho position of the pendant thiophene ring and that of the phenyl unit of the fluorenyl core is the main reason for the observed rotation in the minimal energy configuration calculated for SBF4-DPP.

Similar values of ca 50° have been reported in literature for other 4-subsituted spirobifluorenes.[S2,S4]

Polarized Optical Microscopy

Optical textures were observed with a Leitz Orthoplan polarizing microscopy equipped with a Mettler FP82 hot stage and a FP80 unit.

Differential Scanning Calorimetry and thermogravimetric analysis measurements

DSC curves were obtained with a TA Instruments DSCQ1000 instrument operated at a scanning rate of 5 °C min-1 on heating and on cooling.

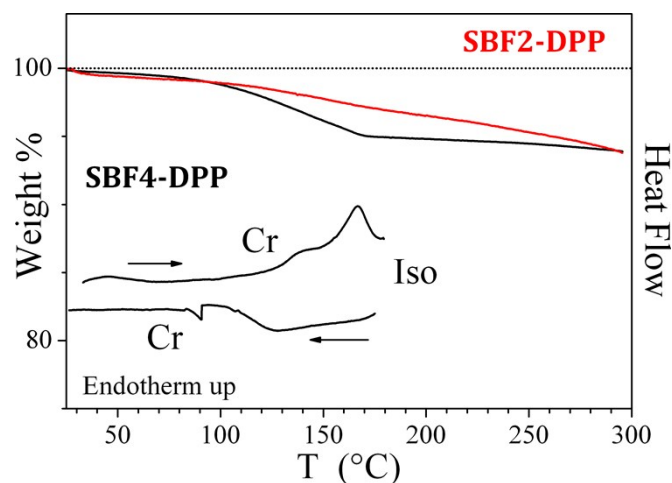The TGA measurements were carried out on a SDTQ 600 apparatus at scanning rate of 10 C min-1.

Figure S4: top: TGA curves of **SBF2-DPP** (red) and **SBF4-DPP** (black); bottom: DSC curve of **SBF4-DPP** with melting transition to isotropic liquid ($\Delta H \approx 4.5$ J/g).

X-Ray diffraction measurements

The SAXS patterns were obtained with a transmission Guinier-like geometry. A linear focalized monochromatic Cu Kα1 beam ($\lambda = 1.5405$ Å) was obtained using a sealed-tube generator (600 W) equipped with a bent quartz monochromator. In all cases, the crude powder was filled in Lindemann capillaries of 1 mm diameter and 10 μm wall-thickness. The diffraction patterns were recorded with a curved Inel CPS120 counter gas-filled detector linked to a data acquisition computer.
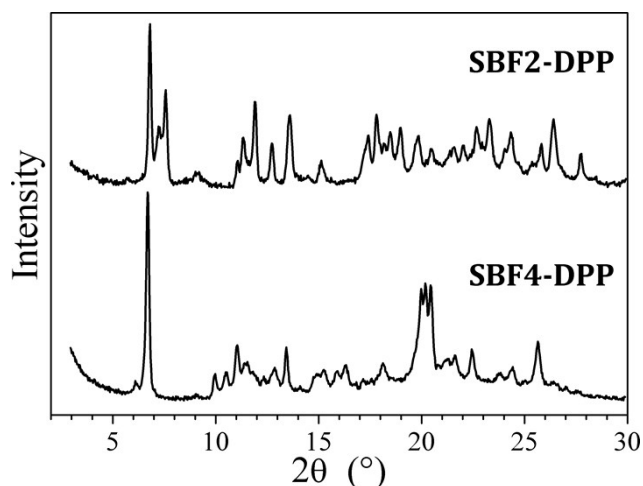

Figure S5: SAXS pattern of **SBF2-DPP** and **SBF4-DPP** at room temperature

Electrochemical measurements.

All electrochemical experiments were performed under an argon atmosphere, using a Pt disk electrode (diameter 1 mm), the counter electrode was a vitreous carbon rod and the reference electrode was a silver wire in a 0.1 M $AgNO_3$ solution in CH_3CN. Ferrocene was added to the electrolyte solution at the end of a series of experiments. The ferrocene/ferrocenium (Fc/Fc+) couple served as internal standard. The three electrode cell was connected to a PAR Model 273 potentiostat/galvanostat (PAR, EG&G, USA) monitored with the ECHEM Software. Activated Al_2O_3 was added in the electrolytic solution to remove excess moisture. For a further comparison of the electrochemical and optical properties, all potentials are referred to the SCE electrode that was calibrated at 0.405 V vs. Fc/Fc^+ system. We estimated the electron affinity (EA) or lowest unoccupied molecular orbital (LUMO) and the ionization potential (IP) or highest occupied molecular orbital (HOMO) from the redox data. The LUMO level was calculated from: LUMO (eV)= -[E_{onset}^{red} (vs SCE) + 4.8] and the HOMO level from: HOMO (eV) = -[E_{onset}^{ox} (vs SCE) + 4.8], based on an SCE energy level of 4.8 eV relative to the vacuum.[S5] The electrochemical gap was calculated from: ΔE_{el} =|HOMO-LUMO| (in eV).
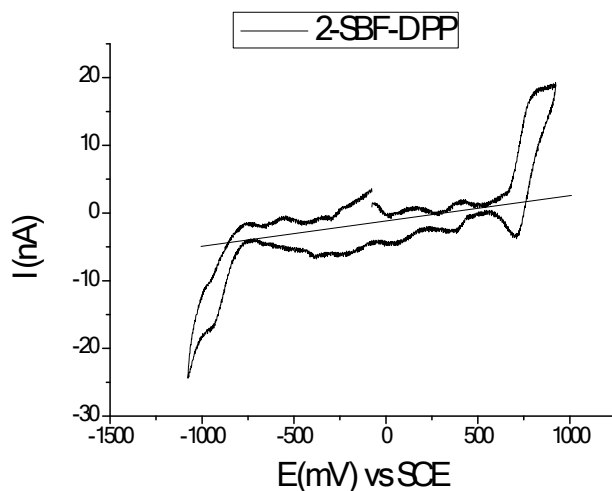

Figure S6: Cyclic voltammogram of **SBF2-DPP** recorded in CH_2Cl_2 + 0.2 M [NBu$_4$][PF$_6$]. Platinum disk working electrode Ø 1mm, sweep-rate: 100 mV/s.

Figure S7: Cyclic voltammogram of **SBF4-DPP** recorded in CH_2Cl_2 + 0.2 M [NBu$_4$][PF$_6$]. Platinum disk working electrode Ø 1mm, sweep-rate: 100 mV/s.
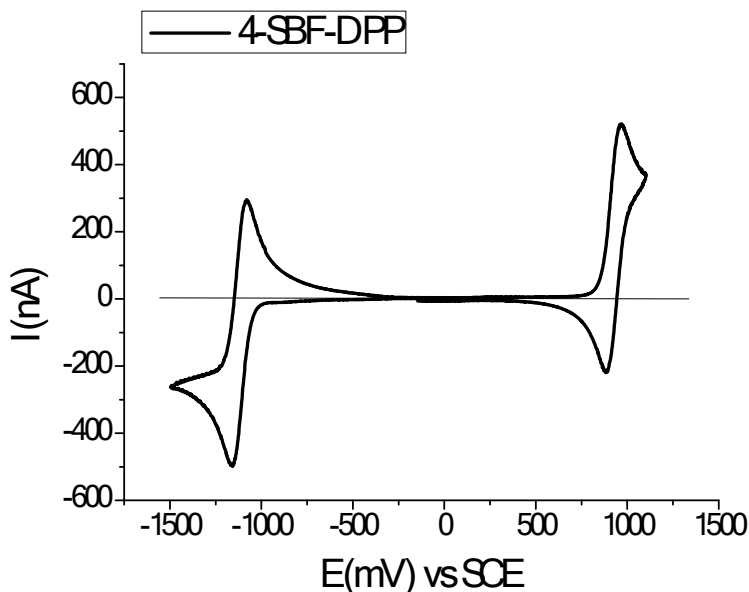
Field effect mobility measurements.

Bottom contact field-effect transistors (FETs) were elaborated on commercially available pre-patterned test structures whose source and drain contacts were composed of a 30 nm thick gold layer on top of a 10 nm thick Indium Tin Oxide (ITO) layer. A 230 nm thick silicon oxide was used as gate dielectric and n-doped ($3x10^{17}.cm^3$) silicon crystal as gate electrode. The channel length and channel width were 20 μm and 10 mm, respectively. The test structures were cleaned in acetone and isopropyl alcohol and subsequently for 30 minutes in an ultra-violet ozone system. Then, hexamethyldisilazane (HMDS) was spin coated (500 rpm for 5 s and then 4000 rpm for 50 s) under nitrogen ambient and followed by an annealing step at 130°C for 10 minutes. Finally, 5 mg/mL anhydrous chloroform of dyes **SBF2-DPP** and **SBF4-DPP** solutions were spin coated (1250 rpm for 60s and 2250 rpm for 60s) to complete the FET devices. The samples were then left overnight under vacuum ($<10^{-6}$ mbar) to remove residual solvent traces. Both, the FET elaboration and characterizations were performed in nitrogen ambient. The transistor output and transfer characteristics were recorded using a Keithley 4200 semiconductor characterization system. The charge carrier mobility was extracted in the linear regime using the usual formalism on FET devices annealed at the same temperature as the optimized photovoltaic devices.

Space-charge-limited current devices.

Hole-only SCLC devices were elaborated to investigate the out-of-plane mobility. The device structure was the following: ITO/PEDOT:PSS/dye/PEDOT:PSS/MoO3/Ag. Highly conductive poly(3,4-ethylenedioxythiophene): polystyrene-sulfonate (PEDOT:PSS) was used as hole injection electrodes. Indium tin oxide (ITO) coated glass with a sheet resistance of 20 Ω/sq was used as substrate. The ITO layer was cleaned sequentially by ultrasonic treatments in acetone, isopropyl alcohol and deionized water. After an additional 30 minutes exposure to ultra-violet generated ozone, a 40 nm thick PEDOT:PSS layer was spin-coated from an aqueous solution on top of the ITO layer and dried for 30 min at 140°C. Chloroform dye solutions of varying concentration were prepared and stirred at room temperature for 24h before spin-coating on top of PEDOT:PSS. The resulting dye layer thickness ranged from approximately 80 nm (for the less dense solution) to 200 nm. The devices were completed by thermal evaporation of 7 nm molybdene oxide and 120 nm silver as top electrode. Device elaboration and characterization were done at room temperature in a nitrogen-filled glove box.

The hole mobility is extracted using the standard expression for charge space limited current density following the Mott-Gurney law:

$$J = \frac{9}{8}\varepsilon_r\varepsilon_0\mu_\text{h}\frac{V^2}{L^3}$$

Where ε_0 is the permittivity of free space, ε_r is the polymer dielectric constant, μ_h is the hole mobility, V is the voltage drop across the device and L is the film thickness.

Photovoltaic conversion measurements.

Bulk heterojunction devices were elaborated using the different synthesized molecules as electron-donor and $PC_{71}BM$ as electron-acceptor. Standard solar cells were elaborated by using the following device structure: ITO/PEDOT:PSS(40nm)/ **SBF2-DPP** or **SBF4-DPP**:$PC_{71}BM$/Al(120 nm). Indium Tin Oxide coated glass with a surface resistance lower than 20 Ω/sq was used as transparent substrate. Substrates were cleaned sequentially by ultrasonic treatments in acetone, isopropyl alcohol, and deionized water. After an additional cleaning for 30 minutes under ultra-violet generated ozone, PEDOT:PSS was spin coated (1500 rpm, 60s) to obtain a 40 nm thick layer and thermally annealed for 30 minutes at 140°C under nitrogen atmosphere. The chlroroform dye:$PC_{71}BM$ solutions were stirred for at least 24 hours at 50°C before spin-coating. An extra stirring for 15 minutes at 100°C was added just before the active layer deposition. The dye **SBF2-DPP** or dye **SBF4-DPP** concentration of the solution was 5 mg/mL. The relative dye **SBF2-DPP** or dye **SBF4-DPP**:$PC_{71}BM$ weight ratio was varied from 1:1 to 1:4. The active layer spin coating conditions were the following: a first 120 seconds

step (speed: 2000 rpm, acceleration: 600 rpm.s) followed by a second 60 seconds step (speed: 2500 rpm, acceleration: 600 rpm/s). Finally, the Al (120 nm) cathode was thermally evaporated. Each device contained four 12 mm^2 diodes, the surface of each diode being carefully defined by a shadow mask. A thermal annealing process (for 10 minutes at 130 and 140°C, for **SBF2-DPP** and **SBF4-DPP** respectively) was added after the cathode thermal evaporation. Current versus Voltage (J-V) characteristics were measured using a source measurement unit Keithley 2400 under darkness and under AM1.5G (100 mW.cm^2) illumination. The standard illumination was provided by a Class A Lot Oriel solar simulator (550 W filtered Xe lamp) and the illumination power was calibrated using a reference silicon solar cell. The photovoltaic cells elaboration after substrate preparation and the characterizations were performed in nitrogen ambient.
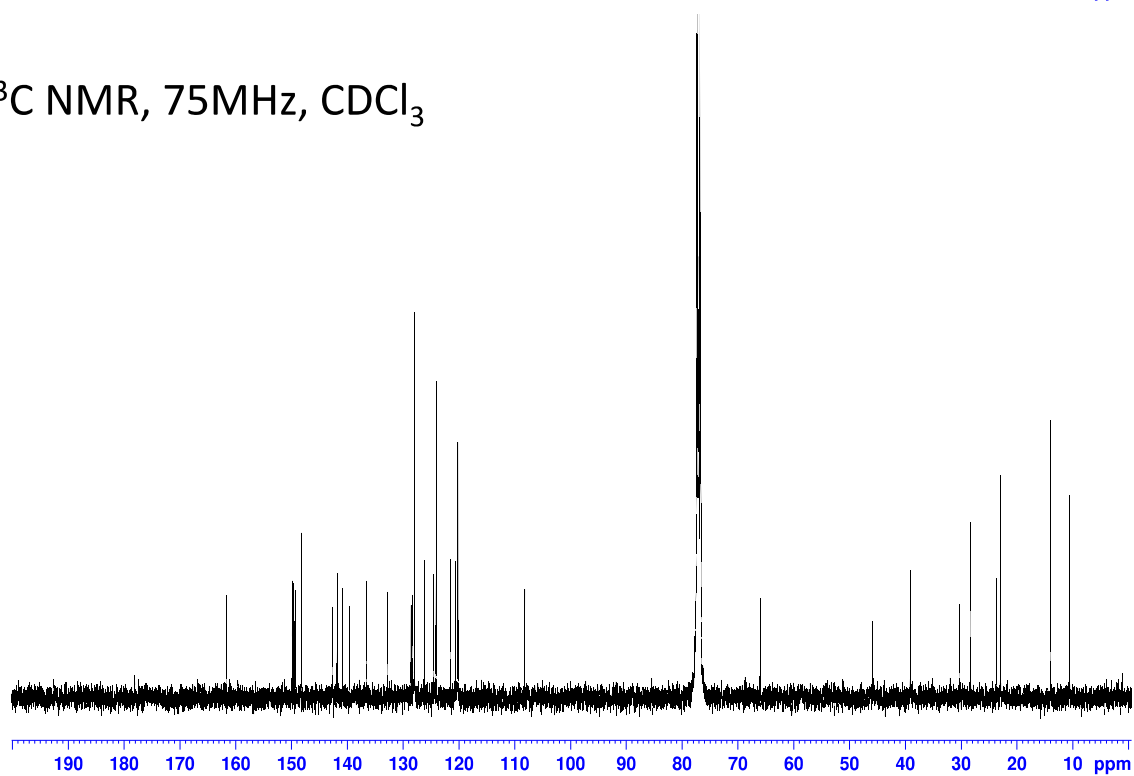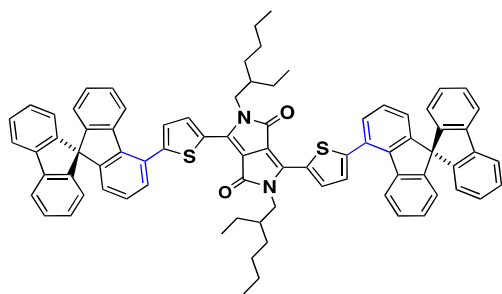
NMR Spectra
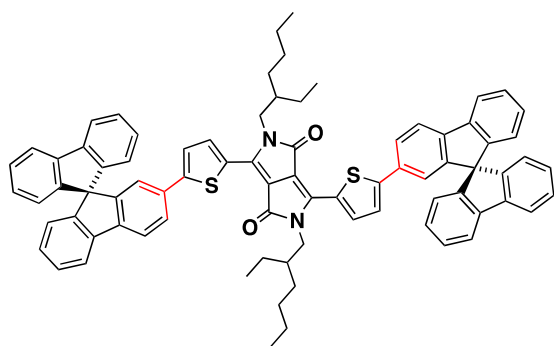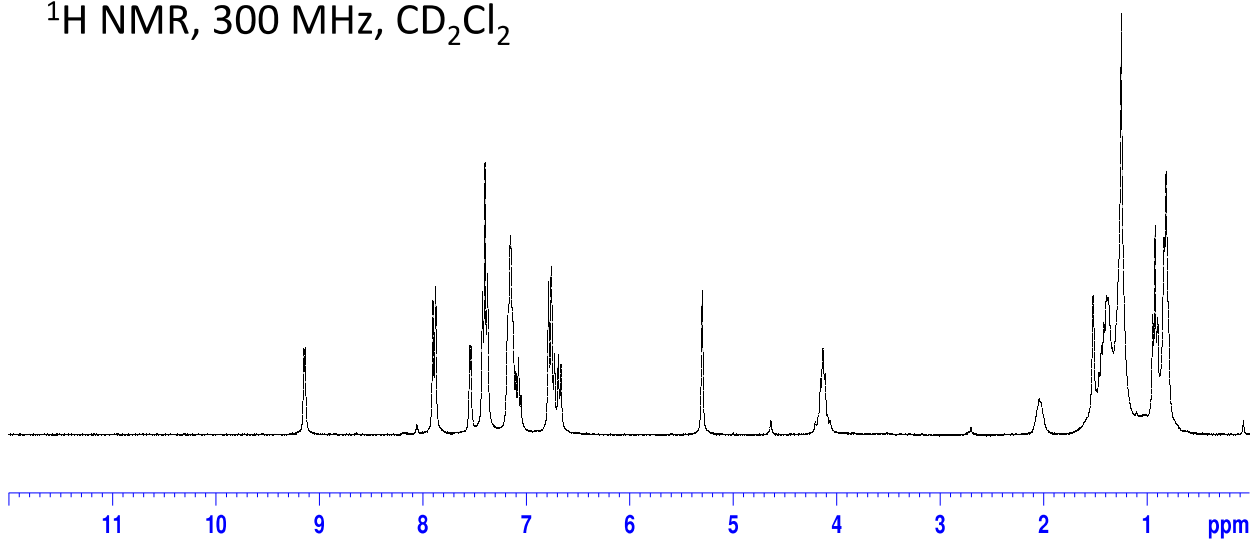
SBF2-DPP

^{1}H NMR, 300 MHz, CDCl$_3$
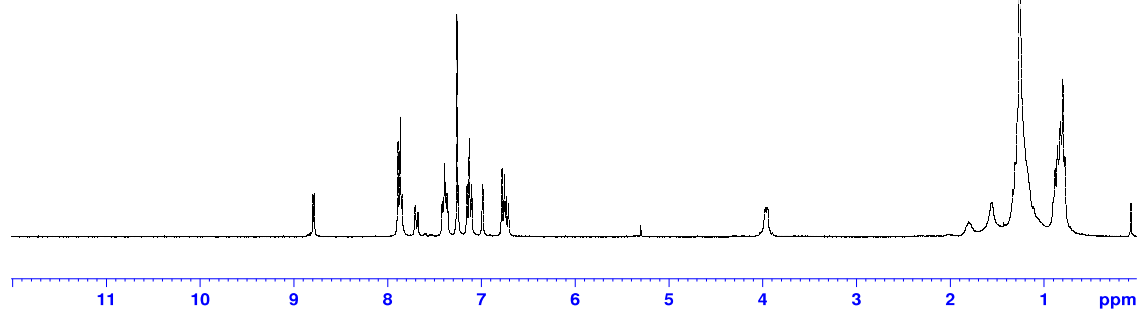
^{13}C NMR, 75MHz, CDCl$_3$
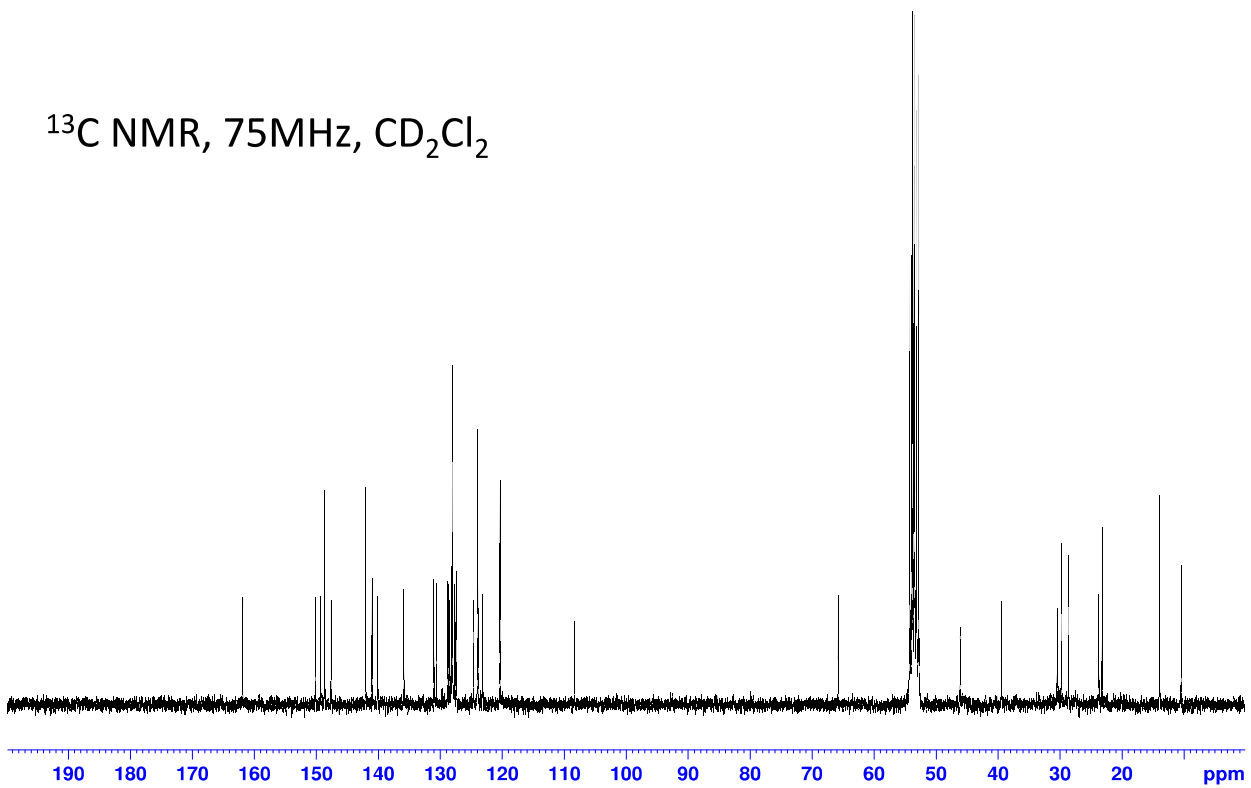
SBF4-DPP

^{1}H NMR, 300 MHz, CD$_2$Cl$_2$

^{13}C NMR, 75MHz, CD$_2$Cl$_2$

References:

S1. T. Bura, N. Leclerc, R. Bechara, P. Lévêque, T. Heiser and R. Ziessel, *Adv. Energy Mater.*, 2013, **3**, 1118.

S2. (a) S. Thiery, D. Tondelier, C. Declairieux, B. Geffroy, O. Jeannin, R. Métivier, J. Rault-Berthelot and C. Poriel, *J. Phys. Chem. C,* 2015, **119**, 5790, (b) Y.-Y. Lyu, J. Kwak, W. S. Jeong, Y. Byun, H. S. Lee, D. Kim, C. Lee and K. Char, *Adv. Funct. Mater.*, 2009, **19**, 420.

S3. S. Thiery, C. Declairieux, D. Tondelier, G. Sea, B. Geffroy, O. Jeannin, R. Métivier, J. Rault-Berthelot and C. Poriel, *Tetrahedron,* 2014, **70**, 6337.

S4. S. Thiery, D. Tondelier, C. Declairieux, G. Seo, B. Geffroy, O. Jeannin, R. Métivier, J. Rault-Berthelot and C. Poriel, *J. Mater. Chem. C,* 2014, **2**, 4156.

S5. J. Pommerehne, H. Vestweber, W. Guss, R. F. Mahrt, H. Bässler, M. Porsch and J. Daub , Adv. Mater., 1995 , **7**, 551.